energies

MDPI

Article

Marine Predator Algorithm (MPA)-Based MPPT Technique for Solar PV Systems under Partial Shading Conditions

Sampath Kumar Vankadara [1], Shamik Chatterjee [1], Praveen Kumar Balachandran [2] and Lucian Mihet-Popa [3,*]

[1] School of Electronics and Electrical Engineering, Lovely Professional University, Phagwara 144001, Punjab, India
[2] Department of EEE, Vardhaman College of Engineering, Hyderabad 501218, Telangana, India
[3] Faculty of Information Technology, Engineering and Economics, Oestfold University College, 1757 Halden, Norway
* Correspondence: lucian.mihet@hiof.no

Abstract: To satisfy global electrical energy requirements, photovoltaic (PV) energy is a promising source that can be obtained from the available alternative sources, but partial shading conditions (PSCs), which trap the local maxima power point instead of the global maxima peak power point (GMPP), are a major problem that needs to be addressed in PV systems to achieve the uninterruptable continuous power supply desired by consumers. To avoid these difficulties, a marine predator algorithm (MPA), which is a bio-inspired meta-heuristic algorithm, is applied in this work. The work is validated and executed using MATLAB/Simulink software along with hardware experimentation. The superiority of the proposed MPA method is validated using four different PSCs on the PV system, and their characteristics are compared to those of existing algorithms. The four different PSC outcomes in terms of GMPP are case 1 at 0.07 s 995.0 Watts; case 2 at 0.06 s 674.5 Watts; case 3 at 0.04 s 654.1 Watts; and case 4 at 0.04 s 364.2 Watts. The software- and hardware-validated results of the proposed MPA method show its supremacy in terms of convergence time, efficiency, accuracy, and extracted power.

Keywords: maximum power point tracking; solar photovoltaics; meta-heuristic algorithm; partial shading conditions

Citation: Vankadara, S.K.; Chatterjee, S.; Balachandran, P.K.; Mihet-Popa, L. Marine Predator Algorithm (MPA)-Based MPPT Technique for Solar PV Systems under Partial Shading Conditions. *Energies* **2022**, *15*, 6172. https://doi.org/10.3390/en15176172

Academic Editors: Sachin Mishra, Wei-Hsin Chen, Epari Ritesh Patro, Jean-Nicolas Louis, Javed Dhillon, Ali Torabi Haghighi and Antonio Caló

Received: 1 August 2022
Accepted: 22 August 2022
Published: 25 August 2022

1. Introduction

In recent times, renewable energy sources (RES) have begun to play a dynamic role in the generation of electricity to meet power demands. The core reasons behind these power demands are industrial growth, commercial utilization, and electric vehicle transportation [1]. Among the various RES, solar PV energy is the best source to cover every one of the aforementioned energy demands [2]. Solar technologies convert sunlight energy into electricity through PV, and the costs of PV systems will significantly decrease due to developments in technology [3]. This technology is risk-free to environmental conditions and is eco-friendly and pollution-free compared to non-renewable resources such as oil, nuclear energy, and gas as well as to the applications of those energy sources, such as solar vehicles, streetlights, irrigation systems, etc. [4]. To carry out the required operations and to obtain the output, MPPT with a DC-DC converter is needed, and an advanced method is proposed in this paper, as shown in Figure 1. Although solar PV systems face inevitable challenges under varying environmental conditions, PSCs are the most influential factors affecting the characteristics of a PV system [5]. The effects of PSCs can be mitigated through different types of maximum power point tracking (MPPT) techniques, which are types of conventional and soft computing techniques that have been addressed in articles [6,7].

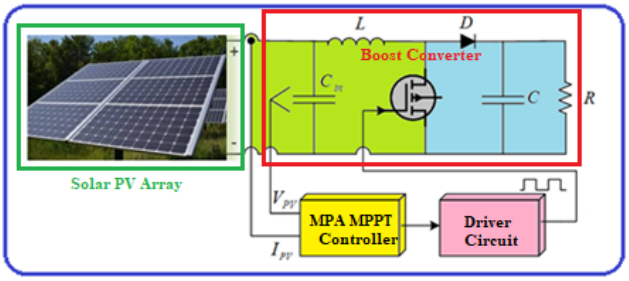

Figure 1. Photovoltaic (PV) system block diagram.

Due to maximum power point (MPP)oscillations, existing techniques such as perturb and observe (P&O) [8], open-circuit voltage tracking (OCVT), incremental conductance (InC) [9], short-circuit current tracking (SCVT) [10], etc., are able to track MPP under uniform conditions since the P-V curve only has one peak. However, these same techniques fail to track MPP under PSC since the P-V curve has multiple peaks.

To overcome this issue of MPPT in PSCs, researchers have developed advanced soft computing techniques such as artificial neural networks (ANN) [11], fuzzy logic (FLC) [12], etc. These advanced intelligent techniques overcome the issues that occur when using existing techniques; however, these approaches encounter several challenges in terms of design, cost, and operation. Furthermore, improper design leads to more tracking time requirements as well as less optimized output in terms of power. To mitigate the mentioned issues, several researchers are currently working on bio-inspired techniques that belong to a group of soft computing techniques known as meta-heuristic algorithms [13]. These bio-inspired algorithms consist of a variety of categories, including particle swarm optimization (PSO) [14], artificial bee colony (ABC) [15], ant colony (ACO) [16], bat algorithm (BAT) [17], cat swarm optimization (CSO) [18], differential evolution (DE) [19], firefly (FA) [20], and grey wolf optimization (GWO) [21], among others. The aforementioned algorithm-based techniques have the capability to find the MPP without any oscillations in the steady-state conditions and can easily determine the global maximum power point (GMPP) using various local maximum power points (LMPPs) while achieving a high level of accuracy.

A new method that not only uses MPA for maximum power point tracking, but that uses two optimization methods for obtaining the MPP: MPA and the mayfly optimization algorithm (MFA), has been proposed. However, this work uses MPA alone, which produces optimal output in terms of time to reach GMPP [22]. Similarly, another method with the same objective that does not use the MPA technique alone to obtain the MPP is a modified MPA method that integrates an opposition-based learning (OBL) strategy with the grey wolf optimizer (GWO), termed MPAOBL-GWO. The proposed MPA does not use any other techniques to improve the swarm agent's local efficiency or to prevent searching deflation. This makes the system very complicated, and to avoid that, we have proposed a simple and effective method to attain the objective [23]. There are a few other studies that have been published in the literature in the same field of research covering topics such as event-trigger-based distributed cooperative energy management for multi-energy systems [24]; integrated energy systems [25]; energy cooperation optimization [26]; and sensorless hybrid MPPT algorithms based on fractional short-circuit current measurements [27].

On the other hand, these bio-inspired techniques face high complexity in terms of accuracy, tracking time, and efficiency under momentary circumstances. To eradicate these difficulties, this article introduces a new bio-inspired algorithm for the MPPT applications called the marine predator algorithm (MPA). Additionally, this MPA can be used for parameter identification in solar PV models since it allows an additional degree of freedom to change the position speed by changing the order of the derivative.

The most important contributions of this article are as follows: 1. The design and analysis of a solar PV system with single-diode and two-diode models under different environmental conditions. 2. The application of MPA for extracting the maximum amount

of generated power during various PSCs. 3. The effectiveness of the proposed MPA-based MPPT is compared to other existing techniques under various PSCs.

The rest of the article is organized as follows: the design of the solar PV system and its characteristics are provided in Section 2. The proposed MPA-based MPPT technique is explained in Section 3, while in Section 4, the results and discussion related to them are conferred, and experimental validation is discussed in Section 5. Finally, the conclusions can be found in Section 6.

2. Modeling of PV Cell and Partial Shading Conditions

2.1. Photovoltaic Module Model

Because of the computational benefits, most PV module models are single-diode models, and recombination loss in the depletion area is often ignored in this type of diode model [28,29]. The equivalent circuit of the PV cell model is shown in Figure 2.

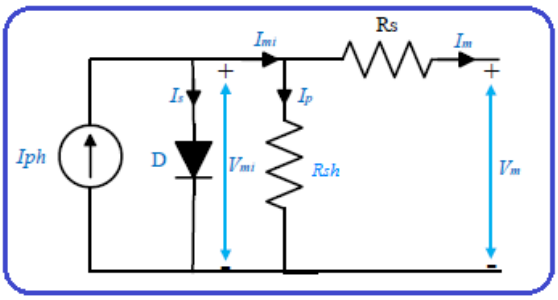

Figure 2. Single-diode PV cell model.

Kirchhoff's current law equation is used to calculate the PV cell's output current. The PV system's current is calculated using the following equation:

$$I = I_{ph} - I_o\left[e^{\frac{q(V+IR_s)}{KTA}} - 1\right] - \frac{V + IR_s}{R_{sh}} \quad (1)$$

where the output current of PV is I, the output PV voltage is denoted by V, the PV module's photocurrent is I_{ph}, the diode current is I_d, the diode's reverse saturation current is I_o, the Boltzmann constant is 1.38065×10^{-23} J/K, the electron charge is q ($1.60217646 \times 10^{-19}$ C), the operating temperature (K) is T, the ideality factor of the diode is A, and the series resistance R_S is normally low, and shunt resistance R_{Sh} is normally high.

$$I_{ph} = (I_{sc\_STC} + k_i\Delta T)\frac{G}{G_{STC}} \quad (2)$$

$$I_o = I_{o\_STC}\left(\frac{T_{STC}}{T}\right)^3 e\left[\frac{qE_g}{AK}\left(\frac{1}{T_{STC}} - \frac{1}{T}\right)\right] \quad (3)$$

$$I_{o\_STC} = \frac{I_{sc}}{e\left(\frac{qV_{oc}}{AKT_{STC}}\right) - 1} \quad (4)$$

Under standard test conditions (STC), the light-generated current is I_{SC_STC}; the temperature at T_{STC} is 25 °C per panel; the difference between T and T_{STC} is T in kelvin; the cell surface irradiance is G;G_{STC} is the STC irradiance (1000 W/M^2); the short circuit current coefficient is K_I; the energy bandgap of the semiconductors is E_G; and I_{O_STC}, shown in Figure 3a,b shows the typical irradiation settings characteristics (G_{STC} = 1000 W/M^2). The temperature ranges of a single-diode PV module may operate between 15 and 55 °C (b). Figure 3c,d show the PV module's characteristics at STC 25 °C under various irradiances ranging from 200 W/m^2 to 1000 W/m^2. The figure clearly shows the multiple peaks for various environmental conditions [28].

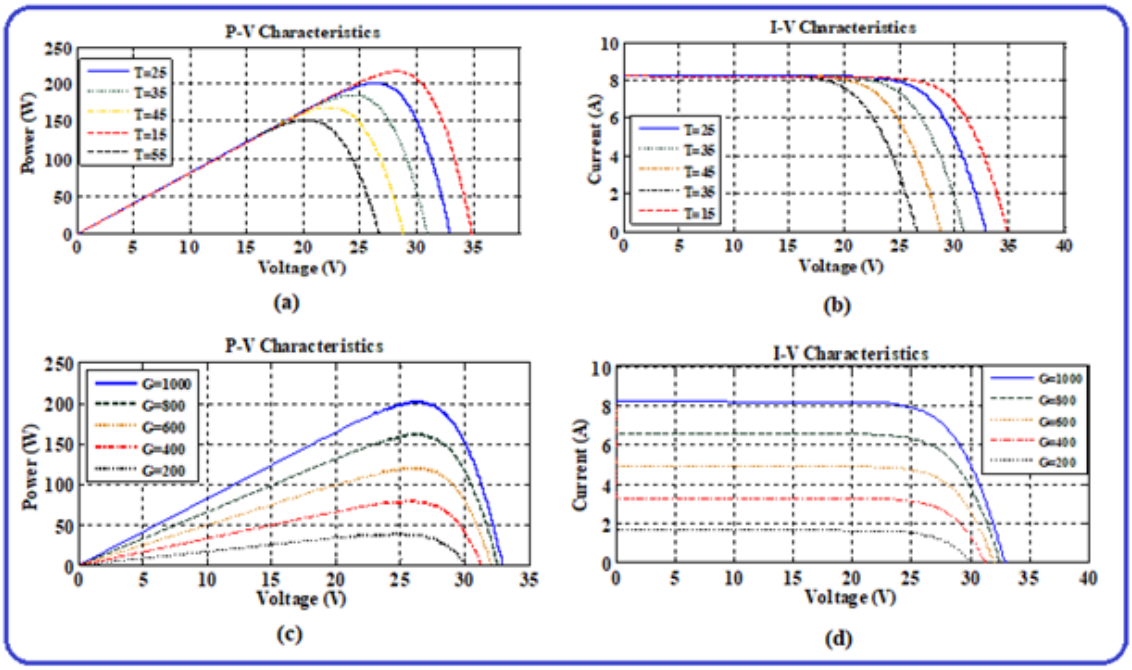

Figure 3. Characteristics of solar PV module at varying temperatures and varying irradiances. (**a**) P-V characteristics at varying temperatures (**b**) I-V characteristics at varying temperatures (**c**) P-V characteristics at varying irradiances (**d**) I-V characteristics at varying temperatures irradiances.

2.2. PV Characteristics under Uniformirradiance and PSCs

A crucial condition in solar PV systems is the partial shading conditions (PSCs). These occur due to varying weather conditions, shadows caused by nearby buildings, passing clouds, trees, dust, and bird waste, among other things [30]. The characteristics of the solar PV under uniform conditions as well as under PSCs are depicted in Figure 4.

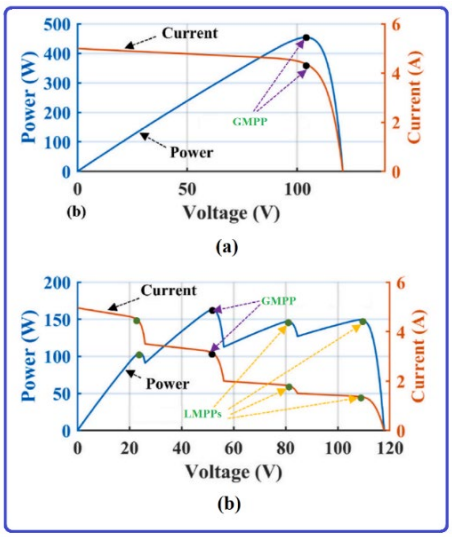

Figure 4. (**a**) P-V and I-V curves during uniform irradiance; (**b**) I-V and P-V curves under PSCs.

As illustrated in Figure 4, the P-V and I-V curves reflect the maximum power point (MPP) during uniform irradiance (a). Partial shading creates a mismatch, which causes hotspots. To reduce hotspot effects, bypass diodes are utilized between modules, which results in many peaks in the P-V and I-V curves, as seen in Figure 4b. As demonstrated in Figure 4, both curves contain LMPPs under the PSCs, with just one being GMPP (b). Solar PV systems should always be operated under GMPP so that the maximum amount of

power produced from solar PV can be collected and transmitted to the load. This article proposes a bio-inspired program dubbed the marine predator algorithm (MPA) to achieve this aim.

3. Methodology

As shown in Figure 1, to carry out the required operation and to obtain the output, MPPT with a DC-DC (boost) converter is needed. The MPPT controller controls a control variable (duty cycle) during MPPT implementation. This produces a control signal in the range of [0, 1], as shown in Equations (5) and (6).

$$V_{out} = \frac{V_{in}}{1 - d} \tag{5}$$

$$d = \frac{T_{on}}{T_{Switching}} \tag{6}$$

where V_{out} and V_{in} are the input and output voltages of the boost converter, and d is the duty cycle. This article introduces a new bio-inspired algorithm based on the marine predator model's social behavior pattern.

3.1. Marine Predator Algorithm

The marine predator algorithm (MPA) is a nature-inspired meta-heuristic optimization technique [31] that has been applied for various optimization problems. Some of the applications of the MPA are estimating the parameters of solar PV cells [32] and COVID-19 image classification [33], among others. In this article, the MPA is applied during MPPT in an optimized way to determine the optimal expected output.

The key points of the MPA are (i) Lévy motion for low-concentration prey environments, (ii) Brownian motion for high-concentration prey environments, and (iii) excellent memory when recalling hunting mates and sites of successful hunting, as depicted in Figure 5. These features make the marine predator's technique more advanced compared to other bio-inspired techniques.

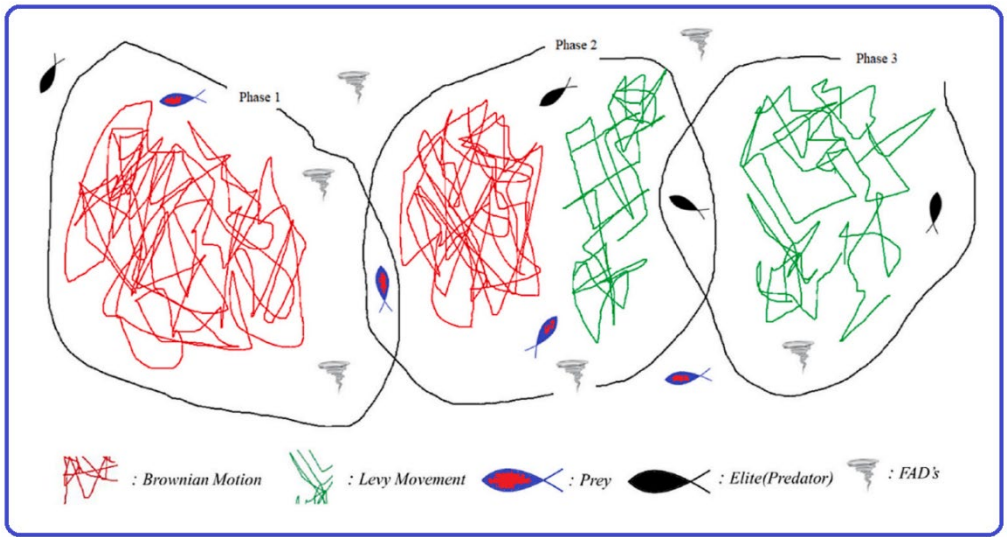

Figure 5. Three phases in marine predator algorithm (MPA) optimization.

3.1.1. Lévy Flight

Lévy flight is nothing but random numbers with step sizes specified by a probability function called Lévy distribution, which is given in Equation (7), where α is theindex distribution, and x and y are the normal distribution variables.

$$\text{Lévy } (\alpha) = 0.05 \times \frac{x}{|y|^{\frac{1}{\alpha}}} \tag{7}$$

3.1.2. Brownian Motion

This probability function is obtained from a normal (Gaussian) distribution, where μ(mean) = 0 and σ^2 (variance) = 1 with step length from a stochastic process called standard Brownian motion. At point x for this motion, the probability density function (PDF) is given by Equation (8).

$$f(x;\ \mu,\ \sigma) = \frac{1}{\sqrt{2\pi}} e^{-\frac{x^2}{2}} \tag{8}$$

3.1.3. Formulation of MPA

Similar to other metaheuristics, MPA is also a population-based technique, in that the first solution is homogeneously spread over the search space as the initial trial. The population can be started by Equation (9), where D_{min} and D_{max} are the variables' lower and higher limits, respectively, while rand is a random integer.

$$D_0 = D_{min} + rand\ (D_{max} - D_{min}) \tag{9}$$

An elite matrix is developed using the fittest solutions among the marine predators based on the "survival of the fittest" theory. Naturally, the topmost predators (denoted by *de*) are brilliant when hunting. The matrix given in Equation (10).

$$Elite = \begin{bmatrix} de_{1,1} & \cdots & de_{1,n} \\ \vdots & \ddots & \vdots \\ de_{m,1} & \cdots & de_{m,n} \end{bmatrix}_{m \times n} \tag{10}$$

Search agents are both predator and prey because both are searching for their food. If the highest predator is replaced by a better predator, Equation (10) is updated, and a new size matrix known as the prey is produced. Accordingly, the position of the predator is updated from time to time. In the prey matrix, $d_{i,j}$ represents the *jth* position of the prey. The prey matrix is given in Equation (11).

$$Prey = \begin{bmatrix} d_{1,1} & \cdots & d_{1,n} \\ \vdots & \ddots & \vdots \\ d_{m,1} & \cdots & d_{m,n} \end{bmatrix}_{m \times n} \tag{11}$$

3.1.4. Optimization Process of MPA

There are three phases of optimization, as shown in Figure 5. Depending on the velocity ratio and time, the phases are classified as follows:

1. Phase 1: Predator moves slower than the prey (velocity ratio is high).
2. Phase 2: Predator and prey are in almost same pace (unity velocity ratio).
3. Phase 3: Predator moves faster than the prey (low velocity ratio).

1. Phase 1: High velocity ratio

If the prey is moving faster than the predator, then this is known as an exploration phase. It only happens in the initial or starting iterations of the algorithm and is given by

Equations (12) and (13). Here, R is the rand [0, 1]. To set a high exploration phase, this phase happens in the first three iterations.

$$\overrightarrow{Stepsize_a} = \overrightarrow{R_B} \times \left(\overrightarrow{Elite_a} - \overrightarrow{R_B} \times \overrightarrow{Prey_a} \right);\ a = i \ldots n \tag{12}$$

$$\overrightarrow{Prey_a} = \overrightarrow{Prey_a} + P\ \overrightarrow{R} \times \overrightarrow{Stepsize_a} \tag{13}$$

2. Phase 2: Unity velocity ratio

This phase imitates both the prey and predator moving at the same pace. To set the explorative and exploitative phases, this phase occurs in the middle of the number of iterations. As such, one population is exploring in one part, and the other population is exploiting in another part, which indirectly depicts exploitation being the responsibility of the predator, whereas responsibility for exploration relies on prey. This phase is represented by Equations (14)–(17), where R_L is the Lévy distribution number or the vector of random numbers based on α.

For the predator population:

$$\overrightarrow{Stepsize_a} = \overrightarrow{R_L} \times \left(\overrightarrow{Elite_a} - \overrightarrow{R_L} \times \overrightarrow{Prey_a} \right); a = i \ldots \frac{n}{2} \tag{14}$$

$$\overrightarrow{Prey_a} = \overrightarrow{Prey_a} + P\ \overrightarrow{R} \times \overrightarrow{Stepsize_a} \tag{15}$$

For the prey population:

$$\overrightarrow{Stepsize_a} = \overrightarrow{R_B} \times \left(\overrightarrow{R_B} \times \overrightarrow{Elite_a} - \overrightarrow{Prey_a} \right); a = \frac{n}{2} \ldots n \tag{16}$$

$$\overrightarrow{Prey_a} = \overrightarrow{Elite_a} + P\overrightarrow{CF} \times \overrightarrow{Stepsize_a} \tag{17}$$

CF is a step size controlling parameter for the predator.

3. Phase 3: Low velocity ratio

In this phase, the prey is moving slower than the predator. To set a high exploitation phase, the Lévy base is a random number. Equations for this phase are given in Equations (18) and (19).

$$\overrightarrow{Stepsize_a} = \overrightarrow{R_L} \times \left(\overrightarrow{R_L} \times \overrightarrow{Elite_a} - \overrightarrow{Prey_a} \right);\ a = 1 \ldots n \tag{18}$$

$$\overrightarrow{Prey_a} = \overrightarrow{Elite_a} + P\overrightarrow{CF} \times \overrightarrow{Stepsize_a} \tag{19}$$

Things that affect the marine eco-system will also affect the marine predators. At times, Eddy formation or fish aggregating devices (FADs) may change the marine predators' behavior. To avoid the FADs, marine predators may make long jumps, as shown in Equation (20), where r1 andr2 are the random indexes of $\overrightarrow{Prey}$ and $\overrightarrow{U}$ is the array of the binary vector [0, 1].

$$\overrightarrow{Prey_a} = \begin{cases} \overrightarrow{Prey_a} + CF\left(\overrightarrow{D_{min}} + \overrightarrow{R} \times \left(\overrightarrow{D_{max}} - \overrightarrow{D_{min}} \right) \times \overrightarrow{U} \right) if r \leq FAD_1 \\ \overrightarrow{Prey_a} + (FAD_s \times (1 - r) + r)\left(\overrightarrow{Prey_{r1}} - \overrightarrow{Prey_{r2}} \right) if r \leq FAD_s \end{cases} \tag{20}$$

3.2. Implementation of MPA for MPPT during PSCs

In the search space between D_{min} and D_{max} [0 to 1], the particles should be initialized for the implementation of MPPT using the MPA optimization technique and should have a population size of four since this work uses four panels in the array. The suggested algorithm will then be used to update all of the initialized particles' locations. Due to irradiance changes, the power (P_{PV}) will change, at which time the code will automatically restart or reinitialize, as shown by the conditional Equation (21).

$$if \ \frac{\left|P_{PV_{new}} - P_{PV_{old}}\right|}{P_{PV_{old}}} \geq P_{PV}(\%) \tag{21}$$

The flow chart of the proposed bio-inspired MPA technique based MPPT is given in Figure 6, which validates Equation (21), and the pseudo-code for the same is also given in the below Algorithm 1.

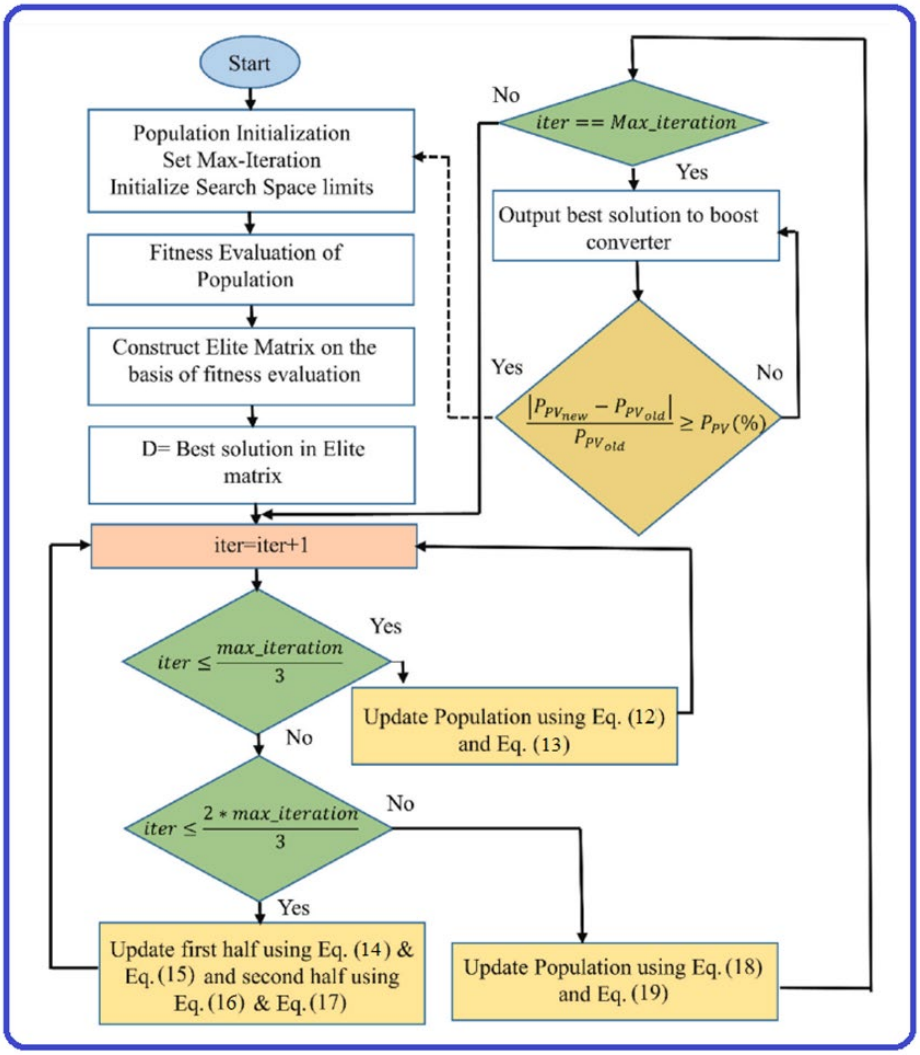

Figure 6. Flowchart for marine predator algorithm-based MPPT.

Algorithm1: MPA-based MPPT Pseudo-code

initialize*the particles* D_i *(i = 1, 2, . . . n)*
while *(iteration < max_iteration)*
evaluate fitness and make Elite matrix
if *(iteration < max_iteration/3)*
update particles using Equations (12) and (13)
else if *((max_iteration/3) < iteration < (max_iteration/(3/2)))*
first half of particles updated using (14) and (15)
second half of particles updated using (16) and (17)
else if
update particles using Equations (18) and (19)
end if
update Elite matrix
apply FADs effect and update using Equation (20)
end while
return d_{best}.

4. Results and Discussion

The proposed MPA-based MPPT technique for solar PV systems was developed using MATLAB/Simulink and was tested experimentally. To validate the results, four different partial shading cases were considered, and the technique was also compared to particle swarm optimization (PSO), grey wolf optimization (GWO), and mouth flame optimization (MFO)-based MPPT techniques. Four 250 W solar PV panels connected in a series–parallel configuration were used in this work, and the rating of the panels at standard testing conditions (STC) are given Table 1. Kyocera KC 250GT PV solar modules were used for this work, and the ratings are in Table 1. Table 2 provides the various PSCs used to validate the proposed work.

Table 1. Solar PV module ratings under STC.

Parameter	Rating
Power at MPP (P_{mpp})	250 W
Open circuited voltage (V_{oc})	36.9 V
Short circuited current (I_{sc})	8.81 A
Voltage at MPP (V_{mpp})	30.3 V
Current at MPP (I_{mpp})	8.11 A

Table 2. Four different cases of PSCs for testing.

Cases	Irradiance in W/m^2			
	P11	P12	P21	P22
Case 1	1000	1000	1000	1000
Case 2	400	400	1000	1000
Case 3	500	800	700	1000
Case 4	200	300	700	1000

4.1. Case 1

In case 1, all four modules were given equal irradiance of 1000 W/m^2. The performance characteristics of the array can be checked by measuring the voltage, current, power, and duty. Figure 7 depicts all of the data with respect to time. Three other MPPT techniques were incorporated into the system for comparison, and the four techniques compared were the (1) proposed MPA algorithm technique, (2) the PSO algorithm technique, (3) the GWO algorithm technique, and (4) the MFO algorithm technique. From Figure 7 it is clear that the time required to reach the MPP is 0.07 s and that the efficiency of MPA is 99.82% according

to the proposed MPA technique. Additionally, it is clear that the proposed MPA technique performed better than the other techniques.

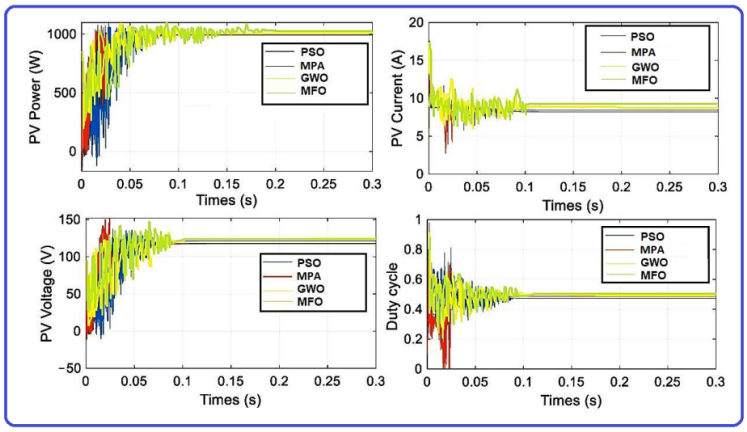

Figure 7. PV power, voltage, current, and duty for MPA, PSO, GWO, and MFO during case 1.

4.2. Case 2

In case 2, all four modules were assigned the variable irradiance values given in Table 2. The performance characteristics of the array could be checked by measuring the voltage, current, power, and duty cycle. Figure 8 depicts all of the data with respect to time. From Figure 8,it is clear that the time required to reach the MPP is 0.06 sand that the efficiency achieved by the proposed MPA technique is 99.86%, which is better than the other three techniques in case 2.

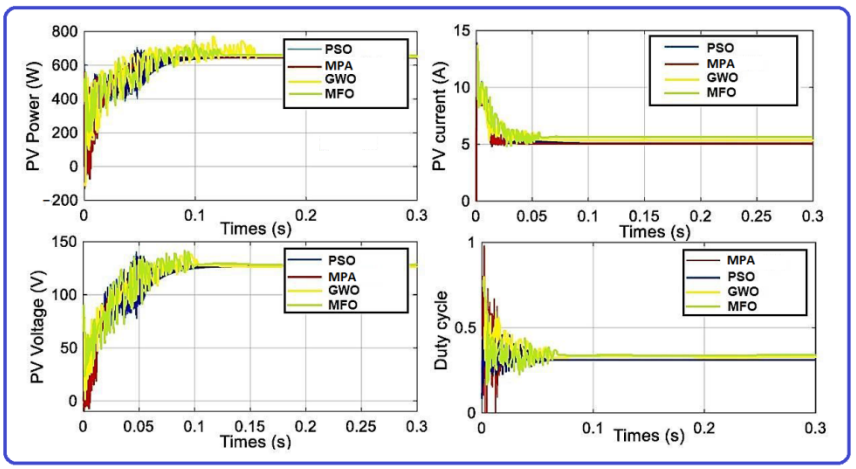

Figure 8. PV power, voltage, current and duty for MPA, PSO, GWO, and MFO during case 2.

4.3. Case 3

Similar to case 2, in case 3, all four modules were given the variable irradiance values given in Table 2. Figure 9 depicts duty data with respect to time, current, voltage, and power. It can be observed that the time required to reach the MPP is 0.04 s and that the efficiency of MPA MPPT is 98.84% when using the proposed MPA technique, which is better than other three techniques in case 3.

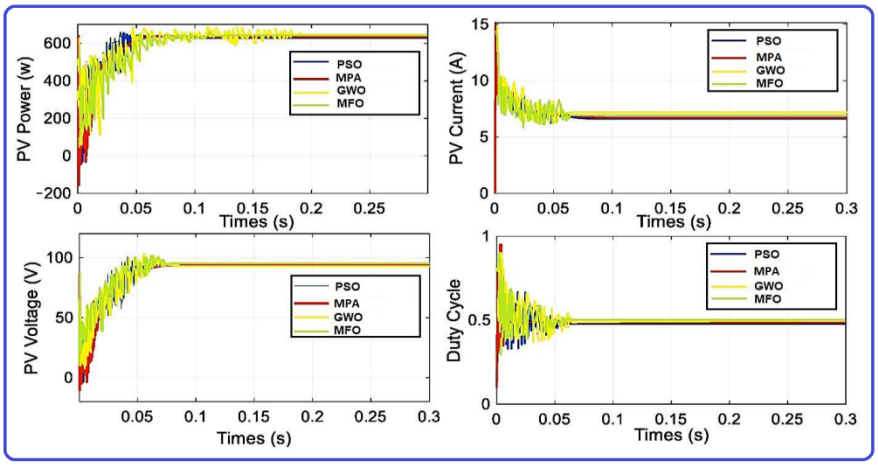

Figure 9. PV power, voltage, current and duty for MPA, PSO, GWO, and MFO during case 3.

4.4. Case 4

Similar to last two cases, in case 4, all four modules were given the variable irradiance values given in Table 2. Figure 10 depicts duty data with respect to time, current, voltage, and power. It can be observed, the time required to reach the MPP is 0.04 s and that the efficiency of MPA MPPT is 98.84% when using the proposed MPA technique, which is better than other three techniques in case 4.

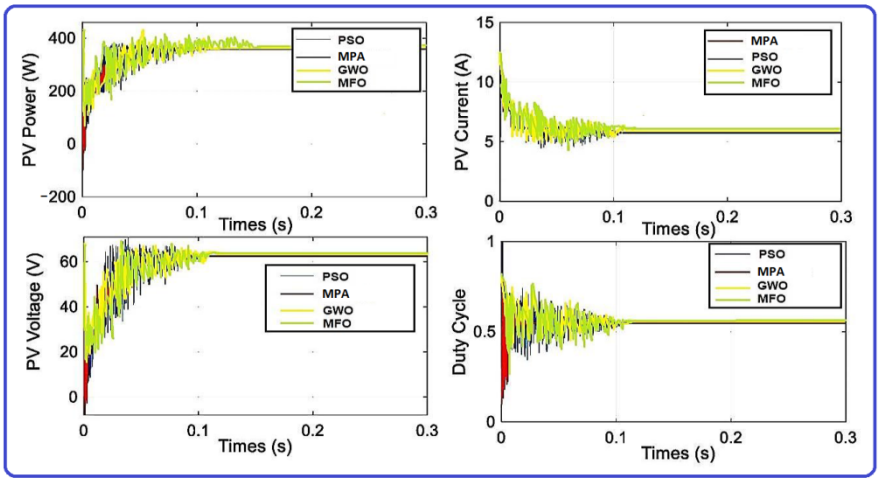

Figure 10. Duty along with PV power, current, voltage for MPA, PSO, GWO and MFO during case 4.

A complete evaluation of the MPA PSO, GWO, and MFO techniques considering four different test cases is given in Table 3. Additionally, the transition during the sudden change in irradiance (case 1 to case 2) is shown in Figure 11. The comparison was carried out by considering power at MPP, the time to attain MPP, and the efficiency of PV. The graph shown in Figure 12 clearly shows that for all the four cases, the MPA technique stays ahead of the other techniques in terms of convergence time. Its efficiency is also almost like that of the best level technique. Moreover, the proposed MPA technique can be easily applied to real-time hardware implementation, but also it needs a sensitive microprocessor such as Pi Zero 2 W.

Table 3. Comparison between MPA, PSO, GWO, and MFO techniques for different test cases.

Performance Parameters	Case 1				Case 2				Case 3				Case 4			
	Various MPPT Techniques															
	MPA	PSO	GWO	MFO	MPA	PSO	GWO	MFO	MPA	PSO	GWO	MFO	MPA	PSO	GWO	MFO
Power extracted at MPP (Watts)	995.0	992.9	995.0	995.2	674.5	672.3	674.6	674.6	654.1	653.8	654.5	654.5	364.2	358.5	364.5	364.7
Time to attain MPP (seconds)	0.07	0.09	0.12	0.20	0.06	0.10	0.16	0.12	0.04	0.10	0.18	0.12	0.04	0.10	0.12	0.16
Efficiency (%)	99.84	99.76	99.93	100	99.86	99.82	100	100	98.85	98.83	99.99	99.99	99.85	99.45	99.98	100

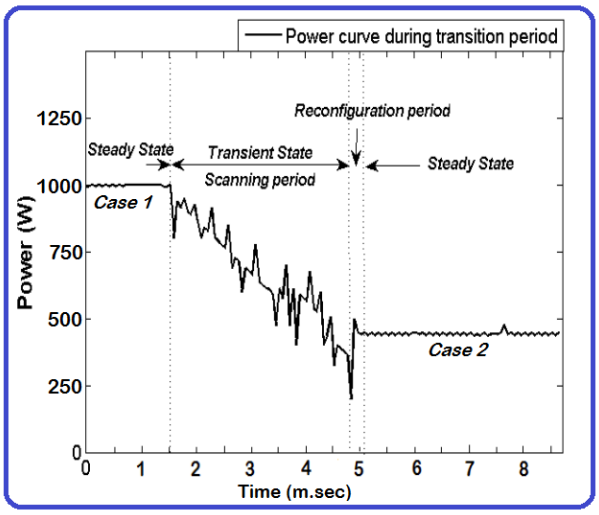

Figure 11. Experimental results of the transient condition from case 1 to case 2.

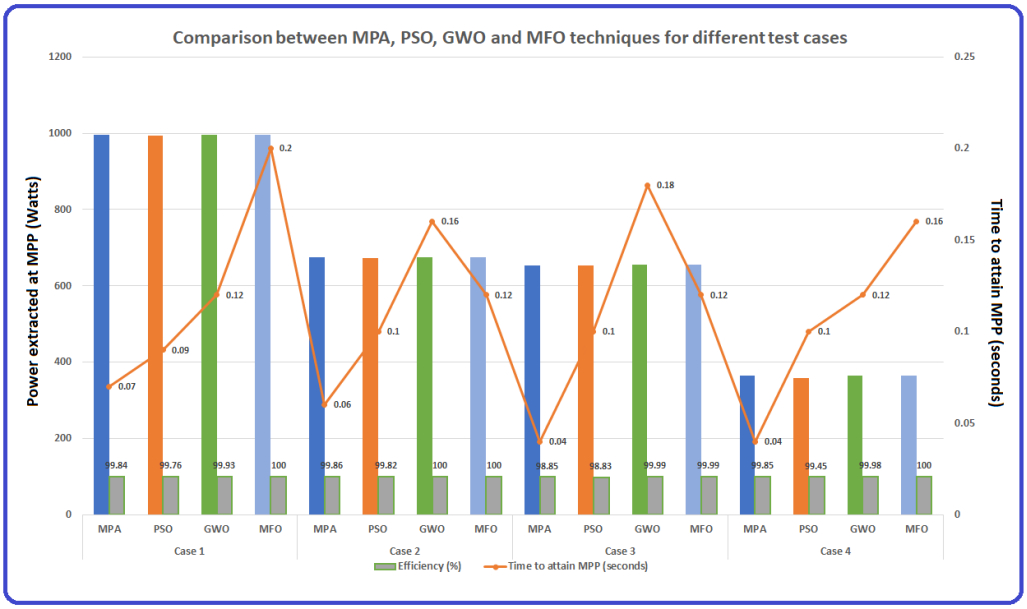

Figure 12. Comparison of MPA, PSO, GWO, and MFO techniques for four different test cases.

5. Experimental Validation

The performance of the proposed MPA method for MPPT was experimentally verified in the four different PSCs cases given Table 2. The suggested MPA approach was applied

in the microcontroller, and the PV simulator simulated the PSC behavior. The results are shown in the following subsections and clearly depict that the performance of the MPA is far better than that of the other techniques.

5.1. Case 1

As described in the simulation, in the first example, uniform irradiation is applied to the PV array, and the time required for GMPP extraction is recorded. Figure 13 clearly shows that the experimental results are closer to the simulation results, which indicates the time taken to achieve GMPP: 0.08 s with 984.55 W.

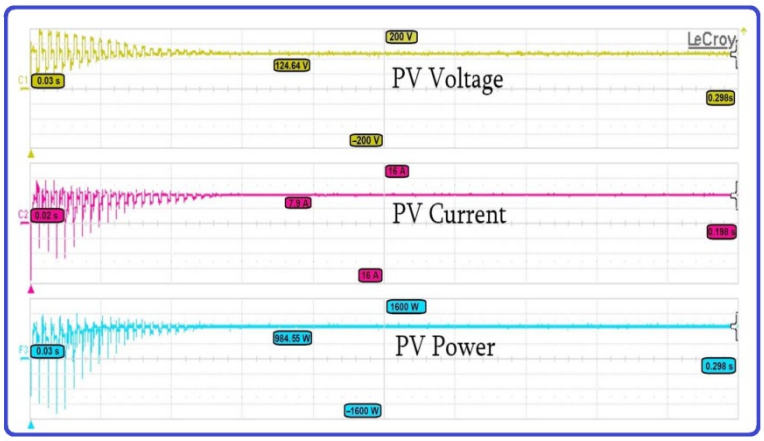

Figure 13. Experimental results of MPA technique for case 1.

5.2. Case 2

Variable irradiations were supplied to the PV array as mentioned in Table 2, and the GMPP extraction time was noted. Figure 14 clearly shows that for case 2, the time taken to achieve GMPP is 0.03 s with 630.39 W at 121.23 V and 5.2 A.

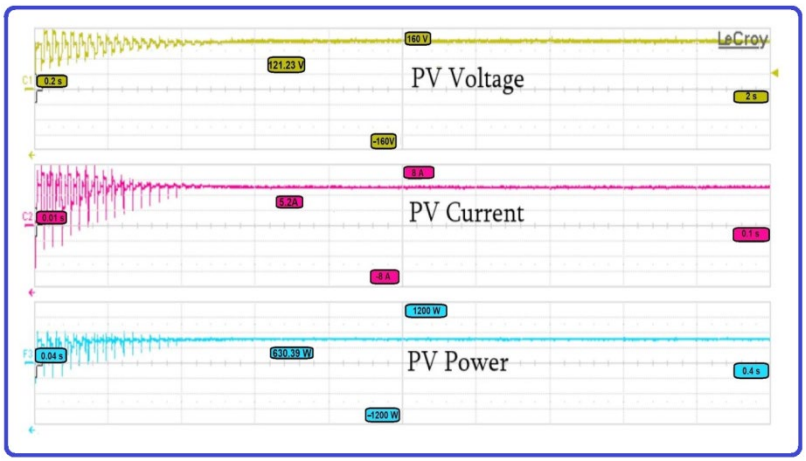

Figure 14. Experimental results of MPA technique for case 2.

5.3. Case 3

For case 3, uneven irradiation values were given to the PV array, and the GMPP extraction time was noted. Figure 15 depicts the time taken to achieve GMPP, which was 0.03 s with 603.66 W, which is similar to the simulation result obtained for the same case.

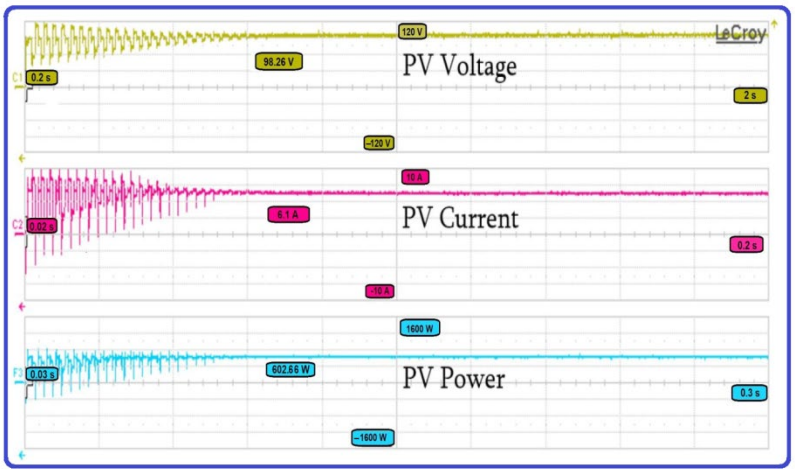

Figure 15. Experimental results of MPA technique for case 3.

5.4. Case 4

Uneven irradiation values were assigned to all of the panels for the PV array in case 4, and the time taken for GMPP extraction was noted. Figure 16 shows the results for case 4, in which the time taken to achieve GMPP was 0.05 s and the respective power was 350.0 W, which is similar to the simulation result obtained for the same case.

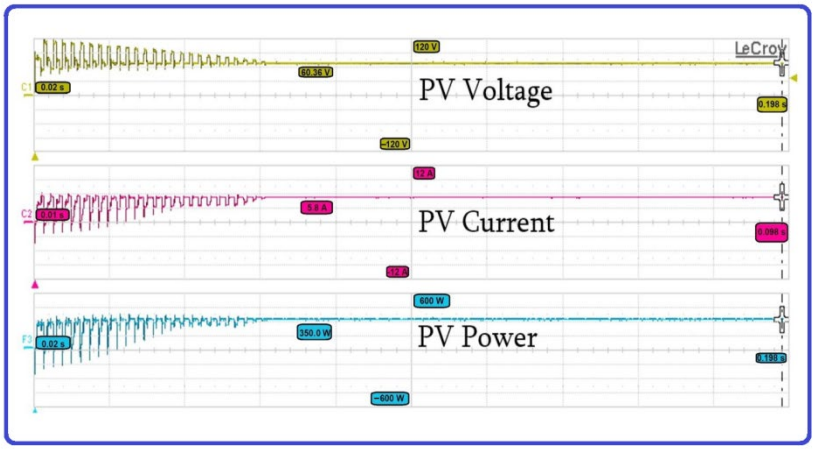

Figure 16. Experimental results of MPA technique for case 4.

6. Conclusions

To track the MPP of a solar PV panel with high accuracy, a bio-inspired algorithm called the marine predator algorithm, which uses a pulse width modulation control boost converter, was applied in this article. To show the effectiveness of the MPA technique, the efficiency, power at MPP, and the time to track MPP for various PSCs were determined. The results show a high degree of MPP tracking accuracy in the steady state with the MPA technique compared to the PSO, GWO, and MFO techniques. The superiority of the proposed MPA method was validated using four different PSCs on the PV system, and its characteristics were compared to those of existing algorithms. The outcomes of the four different PSCs in terms of GMPP are case 1 at 0.07 s 995.0 Watts, case 2 at 0.06 s 674.5 Watts, case 3 at 0.04 s 654.1 Watts, and case 4 at 0.04 s 364.2 Watts. In future work, the effects of partial shading on PV arrays will be tested using more meta-heuristic algorithms, and we will integrate them into the grid via an inverter to be analyzed. Additionally, parameter estimation using MPA will be incorporated to large scale PV systems.

Author Contributions: Data curation, S.K.V.; Formal analysis, S.C.; Investigation, S.K.V. and P.K.B.; Methodology, S.K.V. and P.K.B.; Project administration, S.C. and L.M.-P.; Resources, L.M.-P.; Supervision, L.M.-P.; Visualization, S.C.; Writing—original draft, S.K.V. and P.K.B.; Writing—review & editing, P.K.B. and L.M.-P. All authors have read and agreed to the published version of the manuscript.

Funding: This research received no external funding.

Institutional Review Board Statement: Not applicable.

Informed Consent Statement: Not applicable.

Data Availability Statement: Data sharing not applicable.

Conflicts of Interest: The authors declare no conflict of interest.

References

1. Glöser-Chahoud, S. Industrial disassembling as a key enabler of circular economy solutions for obsolete electric vehicle battery systems. *Resour. Conserv. Recycl.* **2021**, *174*, 105735. [CrossRef]
2. Colak, H.E.; Memisoglu, T.; Gercek, Y. Optimal site selection for solar photovoltaic (PV) power plants using GIS and AHP: A case study of Malatya Province, Turkey. *Renew. Energy* **2020**, *149*, 565–576. [CrossRef]
3. Kittner, N.; Lill, F.; Kammen, D.M. Energy storage deployment and innovation for the clean energy transition. *Nat. Energy* **2017**, *2*, 1–6. [CrossRef]
4. Tsikalakis, A. Review of best practices of solar electricity resources applications in selected Middle East and North Africa (MENA) countries. *Renew. Sustain. Energy Rev.* **2011**, *15*, 2838–2849. [CrossRef]
5. Martínez, D.D.; Codorniu, R.T.; Giral, R.; Seisdedos, L.V. Evaluation of particle swarm optimization techniques applied to maximum power point tracking in photovoltaic systems. *Int. J. Circuit Theory Appl.* **2021**, *49*, 1849–1867. [CrossRef]
6. Balamurugan, M.; Sahoo, S.K.; Sukchai, S. Application of soft computing methods for grid connected PV system: A technological and status review. *Renew. Sustain. Energy Rev.* **2017**, *75*, 1493–1508. [CrossRef]
7. Ovaska, S.J.; VanLandingham, H.F.; Kamiya, A. Fusion of soft computing and hard computing in industrial applications: An overview. *IEEE Trans. Syst. Man Cybern. Part C Appl. Rev.* **2002**, *32*, 72–79. [CrossRef]
8. Elgendy, M.A.; Zahawi, B.; Atkinson, D.J. Assessment of perturb and observe MPPT algorithm implementation techniques for PV pumping applications. *IEEE Trans. Sustain. Energy* **2011**, *3*, 21–33. [CrossRef]
9. Sera, D.; Mathe, L.; Kerekes, T.; Spataru, S.V.; Teodorescu, R. On the perturb-andobserve and incremental conductance MPPT methods for PV systems. *IEEE J. Photovolt.* **2013**, *3*, 1070–1078. [CrossRef]
10. Hadji, S.; Gaubert, J.-P.; Krim, F. Maximum Power Point Tracking (MPPT) for Photovoltaic systems using open circuit voltage and short circuit current. In Proceedings of the 3rd International Conference on Systems and Control, Algiers, Algeria, 29–31 October 2013; pp. 87–92.
11. Almonacid, F.; Rus, C.; Hontoria, L.; Munoz, F.J. Characterisation of PV CIS module by artificial neural networks. A comparative study with other methods. *Renew. Energy* **2010**, *35*, 973–980. [CrossRef]
12. Zhai, P.; Williams, E.D. Analyzing consumer acceptance of photovoltaics (PV) using fuzzy logic model. *Renew. Energy* **2012**, *41*, 350–357. [CrossRef]
13. Basha, C.H.; Rani, C. Different conventional and soft computing MPPT techniques for solar PV systems with high step-up boost converters: A comprehensive analysis. *Energies* **2020**, *13*, 371. [CrossRef]
14. Renaudineau, H. A PSO-based global MPPT technique for distributed PV power generation. *IEEE Trans. Ind. Electron.* **2014**, *62*, 1047–1058. [CrossRef]
15. Oshaba, A.S.; Ali, E.S.; Elazim, S.M.A. PI controller design using ABC algorithm for MPPT of PV system supplying DC motor pump load. *Neural Comput. Appl.* **2017**, *28*, 353–364. [CrossRef]
16. Jiang, L.L.; Maskell, D.L. A uniform implementation scheme for evolutionary optimization algorithms and the experimental implementation of an ACO based MPPT for PV systems under partial shading. In Proceedings of the 2014 IEEE Symposium on Computational Intelligence Applications in Smart Grid (CIASG), Orlando, FL, USA, 9–12 December 2014; pp. 1–8.
17. Da Rocha, M.V.; Sampaio, L.P.; da Silva, S.A.O. Comparative analysis of MPPT algorithms based on Bat algorithm for PV systems under partial shading condition. *Sustain. Energy Technol. Assess.* **2020**, *40*, 100761. [CrossRef]
18. Guo, L.; Meng, Z.; Sun, Y.; Wang, L. A modified cat swarm optimization based maximum power point tracking method for photovoltaic system under partially shaded condition. *Energy* **2018**, *144*, 501–514. [CrossRef]
19. Joisher, M.; Singh, D.; Taheri, S.; Espinoza-Trejo, D.R.; Pouresmaeil, E.; Taheri, H. A hybrid evolutionary-based MPPT for photovoltaic systems under partial shading conditions. *IEEE Access* **2020**, *8*, 38481–38492. [CrossRef]
20. Hemalatha, C.; Rajkumar, M.V.; Krishnan, G.V. Simulation and Analysis for MPPT Control with Modified firefly algorithm for photovoltaic system. *Int. J. Innov. Stud. Sci. Eng. Technol.* **2016**, *2*, 48–52.
21. Mohanty, S.; Subudhi, B.; Ray, P.K. A new MPPT design using grey wolf optimization technique for photovoltaic system under partial shading conditions. *IEEE Trans. Sustain. Energy* **2015**, *7*, 181–188. [CrossRef]

22. Zafar, M.H.; Khan, N.M.; Mirza, A.F.; Mansoor, M. Bio-inspired optimization algorithms based maximum power point tracking technique for photovoltaic systems under partial shading and complex partial shading conditions. *J. Clean. Prod.* **2021**, *309*, 127279. [CrossRef]
23. Houssein, E.H.; Mahdy, M.A.; Fathy, A.; Rezk, H. A modified Marine Predator Algorithm based on opposition based learning for tracking the global MPP of shaded PV system. *Expert Syst. Appl.* **2021**, *183*, 115253. [CrossRef]
24. Li, Y.; Zhang, H.; Liang, X.; Huang, B. Event-Triggered-Based Distributed Cooperative Energy Management for Multienergy Systems. *IEEE Trans. Ind. Inform.* **2019**, *15*, 2008–2022. [CrossRef]
25. Zhang, N.; Sun, Q.; Yang, L.; Li, Y. Event-Triggered Distributed Hybrid Control Scheme for the Integrated Energy System. *IEEE Trans. Ind. Inform.* **2022**, *18*, 835–846. [CrossRef]
26. Rahbar, K.; Chai, C.C.; Zhang, R. Energy Cooperation Optimization in Microgrids with Renewable Energy Integration. *IEEE Trans. Smart Grid* **2018**, *9*, 1482–1493. [CrossRef]
27. Sher, H.A.; Murtaza, A.F.; Noman, A.; Addoweesh, K.E.; Al-Haddad, K.; Chiaberge, M. A New Sensorless Hybrid MPPT Algorithm Based on Fractional Short-Circuit Current Measurement and P&O MPPT. *IEEE Trans. Sustain. Energy* **2015**, *6*, 1426–1434. [CrossRef]
28. Vankadara, S.K.; Chatterjee, S.; Balachandran, P.K. An accurate analytical modeling of solar photovoltaic system considering Rs and Rsh under partial shaded condition. *Int. J. Syst. Assur. Eng. Manag.* **2022**, 1–10. [CrossRef]
29. Brano, V.L.; Ciulla, G. An efficient analytical approach for obtaining a five parameters model of photovoltaic modules using only reference data. *Appl. Energy* **2013**, *111*, 894–903. [CrossRef]
30. Al-wesabi, I.; Zhijian, F.; Shafik, M.B.; Al-Muthanna, G.; Shah, M.A.K.Y. Comparative Study of Solar PV System Performance under Partial Shaded Condition Utilizing Different Control Approaches. *Indian J. Sci. Technol.* **2021**, *14*, 1864–1893.
31. Faramarzi, A.; Heidarinejad, M.; SeyedaliMirjalili, A.; Gandomi, H. Marine Predators Algorithm: A nature-inspired metaheuristic. *Expert Syst. Appl.* **2020**, *152*, 113377. [CrossRef]
32. Soliman, M.A.; Hasanien, H.M.; Alkuhayli, A. Marine Predators Algorithm for Parameters Identification of Triple-Diode Photovoltaic Models. *IEEE Access* **2020**, *8*, 155832–155842. [CrossRef]
33. Sahlol, A.T.; Yousri, D.; Ewees, A.A.; Al-Qaness, M.A.A.; Damasevicius, R.; Elaziz, M.A. COVID-19 image classification using deep features and fractional-order marine predators algorithm. *Sci. Rep.* **2020**, *10*, 15364. [CrossRef] [PubMed]